ANNALI DI GEOFISICA, VOL. 42, N. 3, June 1999

Listening carefully: unique observations of harmonic tremor at Lascar volcano, Chile

Margaret Hellweg
Institut für Geophysik, Universität Stuttgart, Germany

Abstract
During the deployment of Proyecto de Investigación Sismológica de la Cordillera Occidental 94 (PISCO'94) in the Atacama Desert of Northern Chile, a broadband seismic station and a network of three short-period three-component stations were installed around the active volcano Lascar. The resulting data set includes a sequence of harmonic tremor with a fundamental at about 0.63 Hz and up to 30 overtones lasting 18 h. Power spectra and spectrograms of Lascar's harmonic tremor from the various stations demonstrate that the frequencies recorded cannot be explained as path effects, and must therefore be attributed to mechanisms at or near the source. The polarization of the wavefield cannot simply be explained as the propagation of any of the classical types of seismic waves, thus we apply new methods to the data to investigate the narrowband signals of the harmonic peaks. While the amplitude characteristics of these signals cannot be correlated across the network, frequency characteristics of the harmonic wavefield are consistent across stations and components. The tremor's fundamental frequency changes at the same time at all stations, indicating that such changes must be caused at the source. In addition, a change in the frequency of the fundamental, f_1, is reflected exactly in the frequencies of the overtones, nf_1 and peak-broadening in the power spectrum is the result of shifts in the fundamental frequency. It is therefore unlikely that the overtones are produced as resonances. This spectral behaviour indicates rather that the source is some resonance at a single frequency within the magma, magma/gas or gas parts of the volcano whose amplitude exceeds the range for which the assumptions of linear acoustics are valid.

Key words *volcano seismology – harmonic tremor*

1. Introduction

Since Palmieri invented the first seismometer at Vesuvius in 1855, seismological measurements have played an important role in our attempts to understand the physical processes which occur within volcanoes (for a review see Chouet, 1996), as well as our efforts to recognize symptoms which indicate incipient activity (for a review see McNutt, 1996). Many types of volcanic seismic signals are events similar to earthquake records and can be evaluated using techniques developed in earthquake seismology to determine, for example, the location of the source, and other source parameters. Volcanoes, however, also generate other classes of signals for which the tools of earthquake seismology are less effective. Often, however, the onsets of volcanic events are emergent and cannot be used for analysis. Other signals, called volcanic tremor, are usually associated with degassing and continuous processes in the volcano. These signals, which may last for several hours at a time, are generally also emergent and may have stationary frequency signatures. In particular, both tremor and events at volcanoes may have spec-

Mailing address: Margaret Hellweg, Institut für Geophysik, Universität Stuttgart, Richard-Wagner-Straße 44, D-70184 Stuttgart, Germany; e-mail: 112052. 3440@compuserve.com

tra characterized by extremely narrowband peaks. Recently, a subclass of such narrowband signals, having as a signature a spectrum with a fundamental frequency, f_1, and narrow peaks at nf_1, has been recorded using three component, high dynamic range equipment at several volcanoes (for example: Semeru - Indonesia, Hellweg *et al.*, 1994; Lascar - Chile, this study; Galeras - Colombia, Gil-Cruz, 1999; Arenal - Costa Rica, Benoit and McNutt, 1997; and Karymsky, Lees *et al.*, 1997). Studying this data highlights the inadequacy of the methods used in earthquake seismology to derive tremor characterics. We must develop new methods to investigate the wavefield of this unusual tremor, which will allow us to learn about the source.

2. Data

Lascar, a stratovolcano more than 5000 m in altitude, is located on the puna, Chile's altiplano, at 23°22′S, 67°44′W. Gardeweg and Medina (1994) note that it is the most active volcano in Northern Chile. Reports of Lascar's activity began in the sixteenth century with the arrival of the Spanish in the region and have continued to date. Its activity is mainly fumarolic, although the continuous degassing is occasionally interrupted by large explosions from the various craters in the summit region. Since 1986, Lascar has undergone several cycles of lava dome growth and collapse. The growth phases usually last several months and are accompanied by numerous small explosions.

On 19 April 1993, a dome growth phase culminated in the largest historically recorded eruption of Lascar (Bulletin of the Global Volcanism Network (GVN), April, 1993; Gardeweg and Medina, 1994). After several hours of vulcanian explosions, a series of Plinian eruptions generated ash columns and pyroclastic flows (fig. 2.1). This was followed on 20 April 1993, by Strombolian activity. The largest Strombolian fountains were estimated to be about 1.5 km high. In the course of the following month, the eruptive activity declined to the usual level of continuous fumarolic activity with high levels of SO_2 emission. On the average, Lascar emits about 2400 Mg/day SO_2 (Andres and Kasgnoc, 1998).

On 17 December 1993 another, smaller eruption occurred (GVN, March, 1994). After this eruption, the activity decreased to normal levels within several hours. As observed from San Pedro de Atacama between January and May 1994, Lascar's activity was limited to the emission of steam and SO_2 (G. Asch, personal communication). Despite its apparent quiescence during this period, Lascar produced many interesting and unusual seismic signals.

During the deployment of the Proyecto de Investigación Sismológica de la Cordillera Occidental 94 (PISCO'94) in the Atacama Desert of Northern Chile (Asch *et al.*, 1995, 1996), a broadband seismic station (B12) and a network of three, short-period, three-component stations (LA1, LA2, and LA3) were installed in a quadrilateral around the volcano Lascar (Asch *et al.*, 1995). All seismometers are flat to velocity in their passbands. In the following analysis, a Butterworth highpass filter was applied to data from the broadband station (B12) to limit the passband to that of the L-4 seismometers, 1 Hz, and the data were converted to ground velocity using the seismometer's parameters. The data for all other components were converted to ground velocity and unless otherwise stated are unfiltered. The stations are described in table I. The data set includes more than one month of continuous recordings with a dynamic range of 140 dB.

The recordings for 18 April 1994 include unusually regular signals at all four stations (fig. 1). The seismograms shown here have two remarkable features which are characteristic for the entire 18 h interval for which this tremor was recorded. Although the waveforms differ on each component, it is obvious that the repeat time, or period, is the same. During the 30 s interval in fig. 1, the waveform changes very little.

The linear power spectrum at station LA2, exemplified by that of the E-component (fig. 2a) has seven evenly spaced peaks with varying amplitudes. The first peak is located at the frequency f_1 = 0.63 Hz. The other peaks appear to be integer harmonic multiples of this fundamental, leading to the designation harmonic tremor. In a plot of the logarithm of the power (fig. 2b), 14 peaks can be recognized in the

Table I. Station description and parameters.

Station	Coordinates	Site geology*	Dist/Az to crater	Sensor	Gain (Vs/m)		Period (s)
B12	3950 m	At edge of	6.4 km		Z	1500	120
100 Hz	23°19′27″S	lava flow	128°	STS-2	N	1500	120
	67°46′43″W	in ash/tephra			E	1500	120
LA1	4000 m	On E flank of a valley	6.7 km		Z	271.7	0.99
200 Hz	23°23′55″S	near old lava flow,	49°	L4	N	279.9	0.97
	67°46′42″W	buried in ash/tephra			E	285.4	0.98
LA2	4750 m	Near wall of welded	3.5 km		Z	275.2	0.98
200 Hz	23°23′25″S	tuff protected by large	352°	L4	N	285.4	0.98
	67°43′27″W	boulders, in ash/tephra			E	283.5	0.96
LA3	4700 m	Buried in	5.5 km		Z	284.3	0.96
200 Hz	23°19′43″S	ash/tephra	231°	L4	N	275.6	0.97
	67°41′14″W	plain			E	279.1	0.97

* Alex Rudloff (personal communication).

spectrum for station LA2. Logarithmic power spectra for the E-components at the other stations have peaks at precisely the same frequencies, although the amplitude of any given peak varies from one station to another. The amplitudes of the first seven peaks are between 1.5 and 2 orders of magnitude above the noise, while the amplitudes of the next seven peaks have much lower signal-to-noise ratios, only about 0.5 orders of magniude above the noise.

Close inspection of a spectrogram of a two hour interval (fig. 3) reveals that while the harmonic tremor is not disrupted by regional events (arrows), the fundamental frequency does change as a function of time. The frequencies for the overtones change correspondingly, according to the formula $f_n = nf_1$. On the other hand, the amplitudes of the lines (indicated by their brightness) appear to vary more randomly with time. They cannot be described by a relationship of the form $a_n = c_n a_1$, where c_n is a constant for a given overtone. The inset in fig. 3 shows a higher resolution spectrogram for a ten minute subset of the two hour interval. Here the overtones are visible at frequencies above 15 Hz corresponding to $n > 24$.

Unlike earthquake seismograms, harmonic tremor has neither a sharp onset nor clearly distinguishable wavegroups. For short intervals, we can plot the particle motion to determine the polarization of the waves. In fig. 4a, 9.6 s of particle motion of the fundamental in the horizontal plane is plotted on a sketch of the network. In this representation the short-term polarization of the fundamental is inconsistent with an hypothesis of any single one of the standard seismic wave types propagating from a point source through a simple medium to the four stations. Figure 4b shows the particle motion at the station LA2 in the three planes determined by the seismometer. For wavefields of unknown type, the particle motion in the horizontal plane is obviously missing part of the story. It is better to view the particle motion in a three-dimensional representation, as shown in fig. 4c for the first three harmonics at the four stations. Unfortunately, it remains impossible on the basis of this figure alone to characterize the tremor wavefield for these lines as P, S_V, S_H or surface waves.

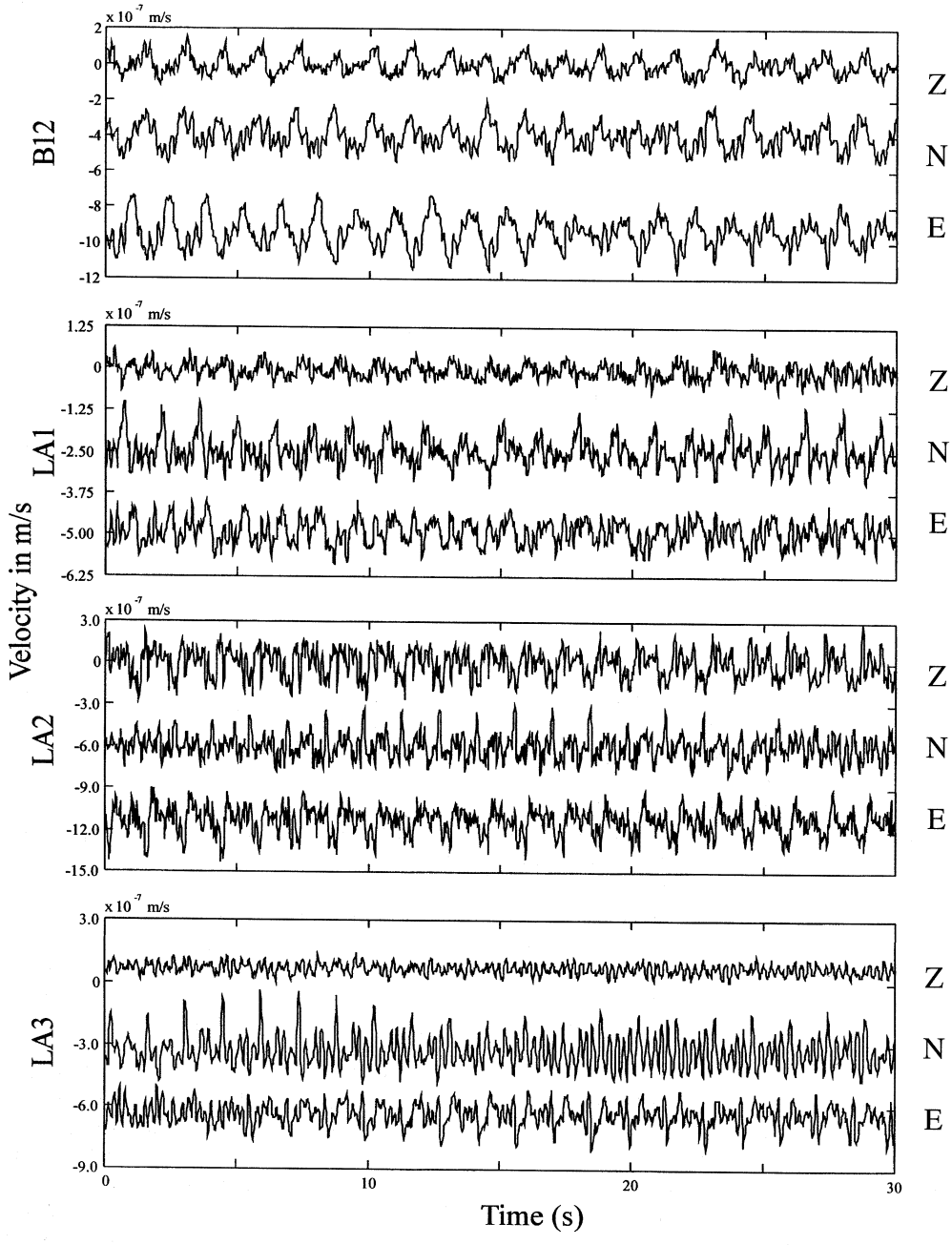

Fig. 1. Thirty seconds of harmonic tremor at all stations. For each station, the N and E traces have been shifted to negative values for clarity. Data from station B12 has been highpass filtered with a corner frequency of 0.5 Hz. All channels were lowpass filtered at 24.5 s and resampled to 50 Hz before analysis.

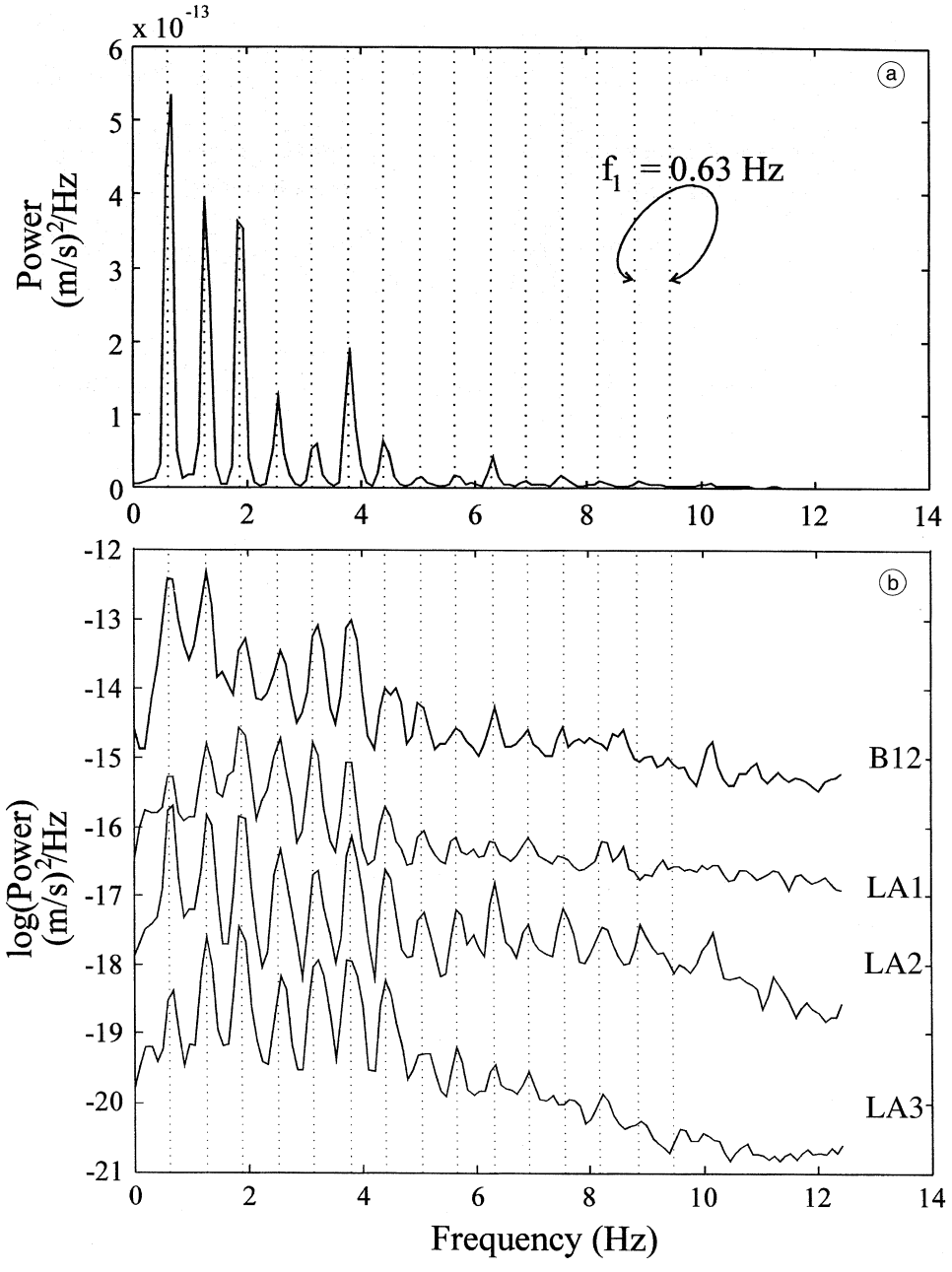

Fig. 2a,b. Power spectrum of harmonic tremor taken from a 600 s interval beginning at 02:35 UTC on 18 April 1994. Power spectra were calculated using 512 point (10.24 s) intervals, with 50% overlapping. Dotted lines are plotted at n*0.63 Hz (n = 1,2,3,...). a) Linear plot of the power spectrum of the E component at station LA2. b) Log-linear plots of the power spectra for the E components at all stations. The traces for LA1, LA2 and LA3 have been shifted for clarity.

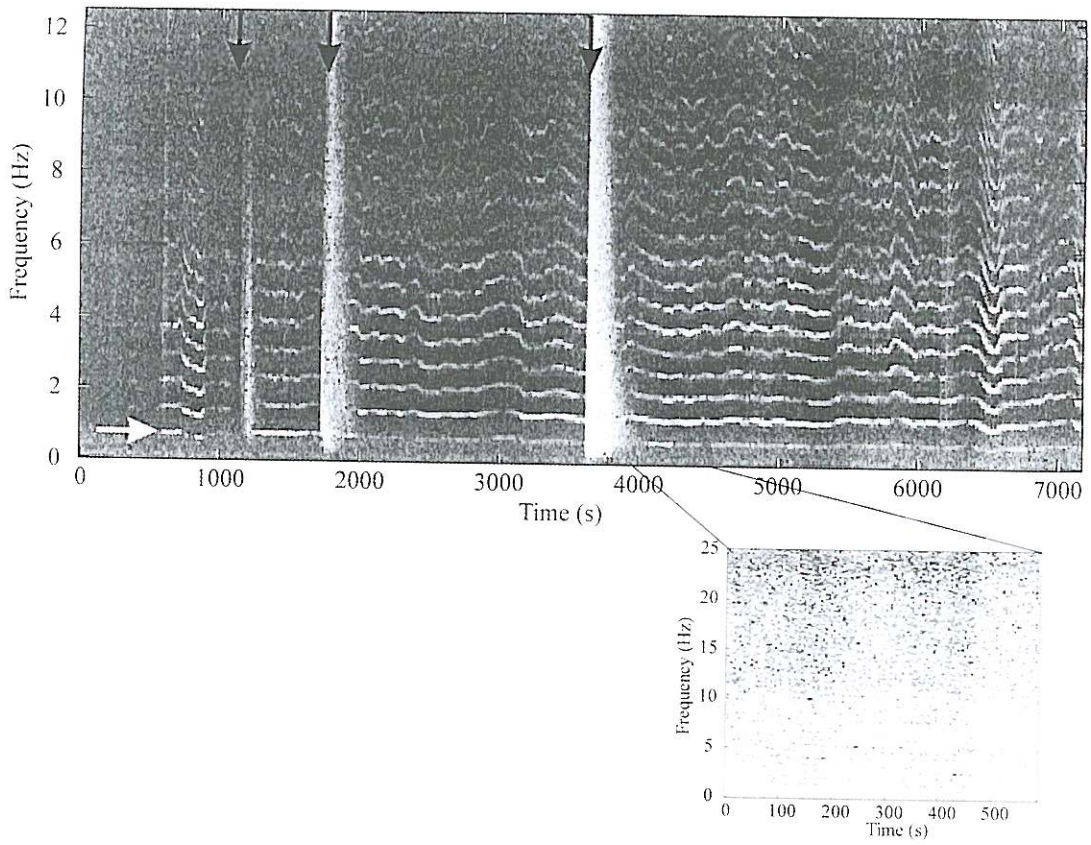

Fig. 3. Spectrogram from 2 h of data from the E component of station LA2 beginning at 01:30 UTC on 18 April 1994. The spectrogram was calculated using 512 point (20.48 s) intervals, with 50% overlapping. Black arrows mark the onsets of three regional events, while the white arrow marks the fundamental. Inset: spectrogram from the E component at station LA2 for the 600 s interval shown in fig. 2a,b. It was calculated using 512 point (10.24 s) intervals with 87.5% overlapping.

3. Analysis

Three characteristics of harmonic tremor signals clearly differentiate them from earthquake waves. It has a relatively stationary pattern of repeating signal shapes, no clear onset and its spectrum contains many evenly spaced, very narrow peaks. The application of traditional earthquake seismological analysis methods to harmonic tremor does not produce useful results. It is thus necessary to apply other tools to study the characteristics of harmonic tremor.

3.1. *Polarograms*

Polarization analysis using particle motion diagrams (fig. 4a-c) can typically be applied only to short data intervals. The question remains whether the polarization stays constant for extended periods during the harmonic tremor episode. Following Matsumura (1981), Seidl and Hellweg (1991) use the covariance matrix of the three-component ground motion recorded in bandpass-filtered seismograms to determine the orientation of the ellipsoid during a short interval. They define the polarization di-

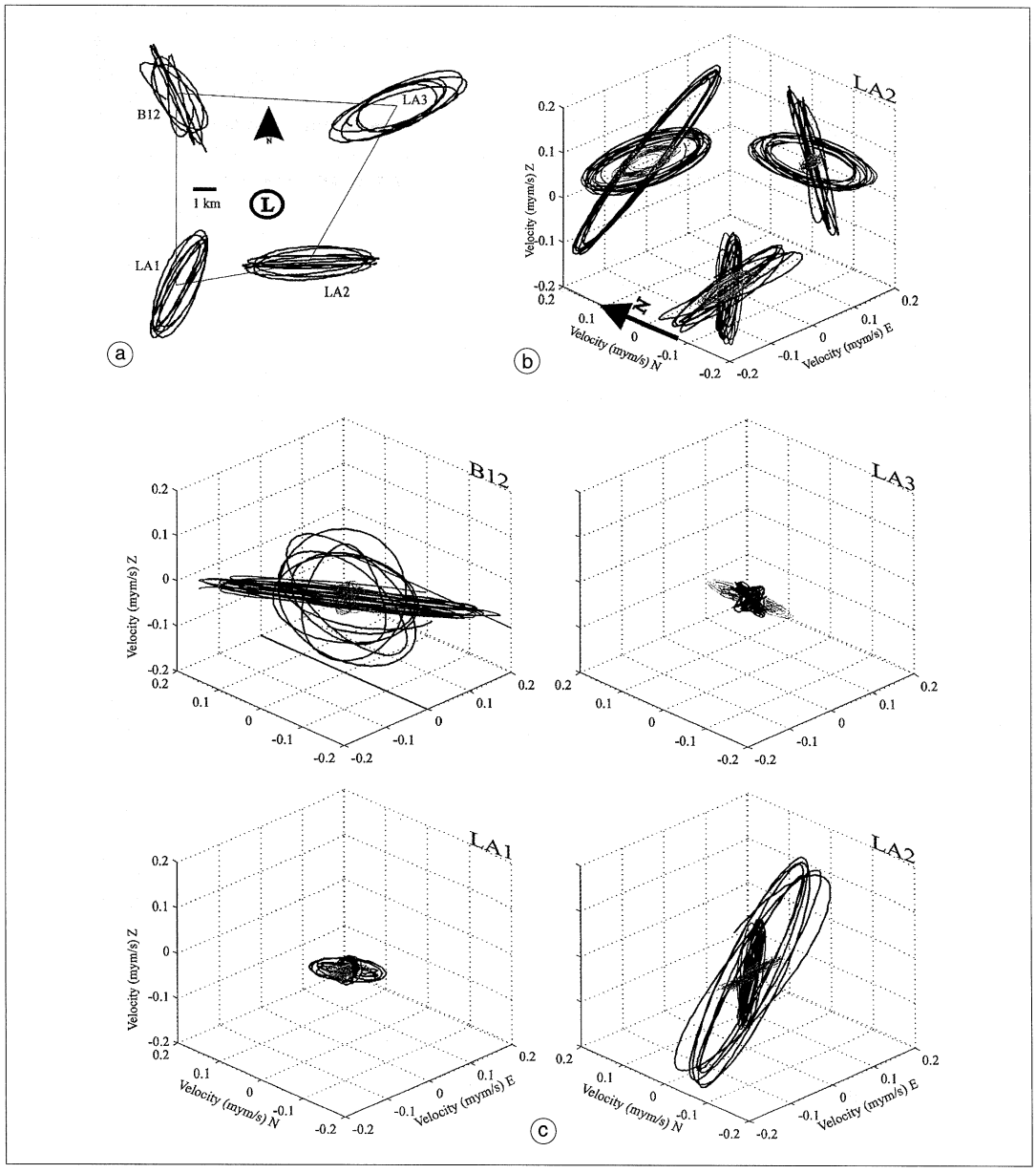

Fig. 4a-c. a) Particle motion in the horizontal plane for 9.6 s of the fundamental (BP limits: 0.5-0.9 Hz) taken from the 600 s interval shown in fig. 2a,b (start time: 02:38:20 UTC). The particle motion diagrams are plotted at their respective station location. L marks the approximate location of the active crater. The quadrilateral sketches the net. b) Particle motion at station LA2 projected into the N-E, Z-N and Z-E planes for the first three spectral lines for the same interval as in (a). The bandpass (BP) limits for the filters are: fundamental (black, 0.5-0.9 Hz), first harmonic (dark gray, 0.9-1.5 Hz), second overtone (light gray, 1.5-2.1 Hz). c) Three-dimensional particle motion at all four stations for the first three spectral lines.

rection (given as an azimuth and inclination) as the direction of the eigenvector belonging to the largest eigenvalue and plot the azimuths for many segments as one histogram. The inclination, measured in the plane defined by the azimuth («R») and the vertical (Z), is plotted as another histogram in the «R»-Z plane. Unfortunately, this representation can be misleading. The difficulty is twofold. The «R» direction for each segment is determined by the azimuth of polarization direction, so that different azimuths may contribute to the same inclination stack. If the waves are not P, S_v or Rayleigh waves, the direction of maximum polarization, designated «R» by Seidl and Hellweg (1991) may not coincide with the direction to the source.

A better represention of the azimuth and inclination of the polarization is given in fig. 5. In a plane defined by all possible azimuths around the compass and inclinations from up (U) through horizontal (H) to down (D), the shading gives the frequency of occurrence. For the fundamental at the station LA2 (fig. 5, lower right), the most frequent particle motion is polarized 70° east with an inclination of 40° up from the horizontal. The polarization of the fundamental at each of the four stations (fig. 5) is summarized in table II. Note that for three of the stations there are two predominant polarization directions during the analysis interval. The polarization for other frequencies is different.

Table II. Polarization of the fundamental.

Station	Azimuth from N	Inclination from H
B12	90°, 60°	0°, 15°
LA1	160°, 10°	10°, – 5°
LA2	70°	40°
LA3	70°, 30°	5°, 5°

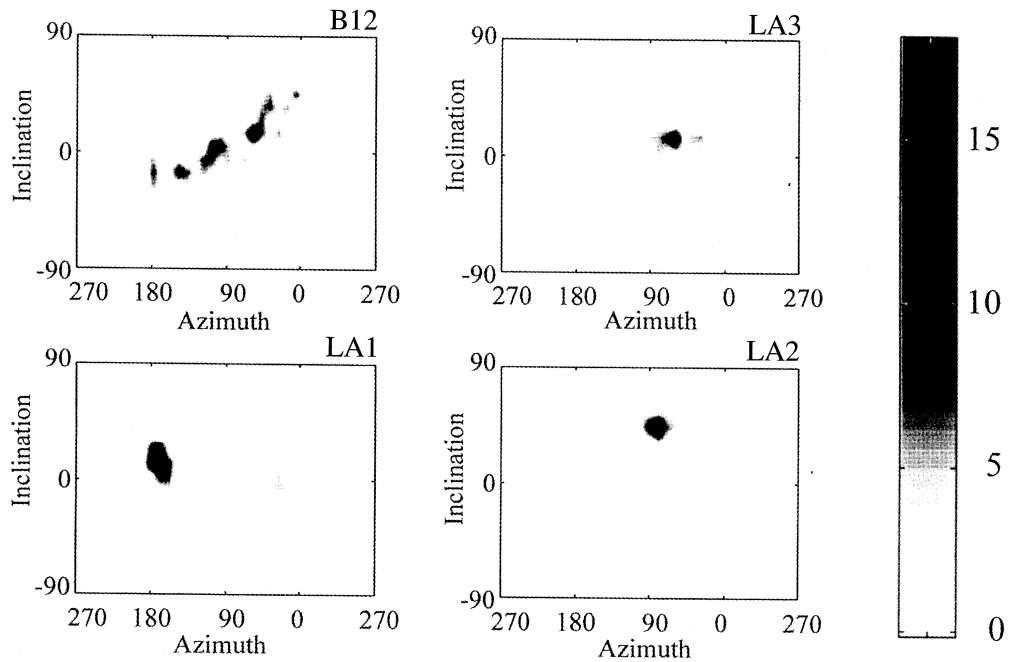

Fig. 5. Polarograms for the fundamental at the four stations (BP filter 0.5-0.9 Hz). The shading gives the frequency of occurrence.

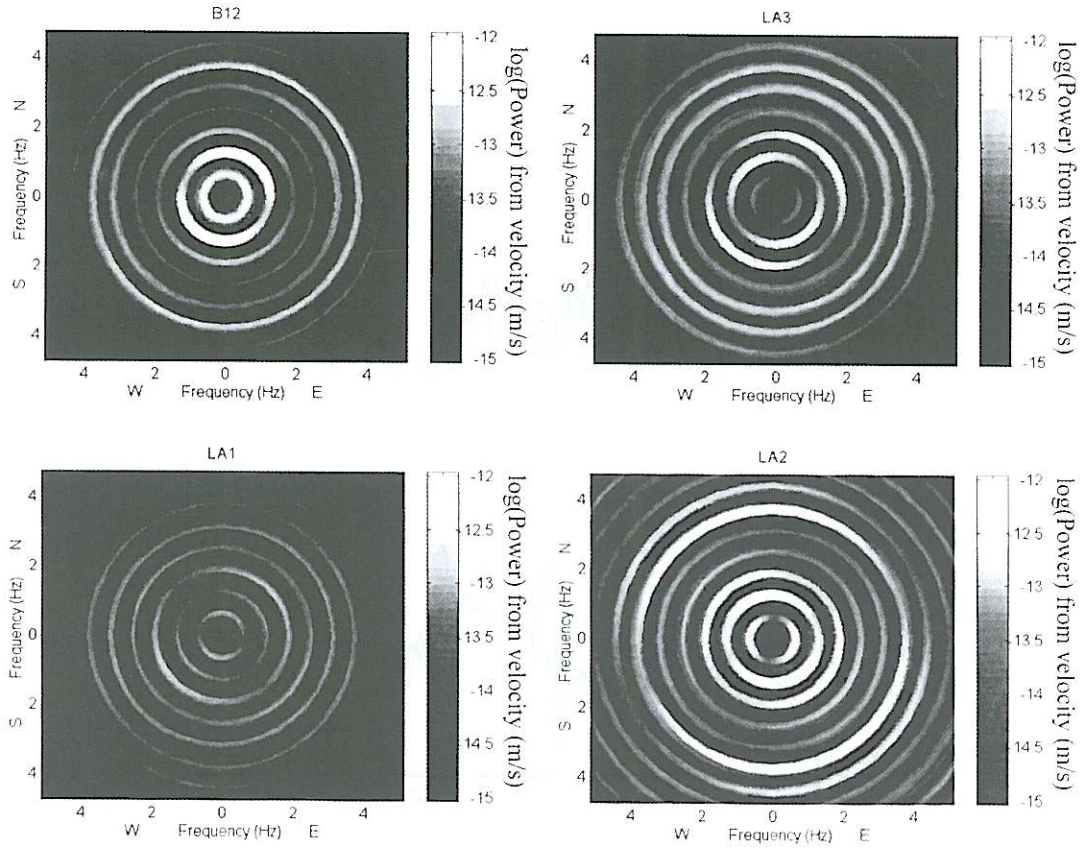

Fig. 6. Directional power for the interval described in fig. 2a,b. Directional power spectra for the horizontal particle motion for the 4 stations. These diagrams show the predominant directions of polarization in the horizontal plane for the first seven harmonics.

3.2. *Directional dependence of the power spectrum*

For the methods of polarization analysis described previously, each spectral line is analyzed separately. It is often desirable, however, to represent the average polarization for several harmonics (or other narrowband signals) at once. This can be accomplished by plotting the directional dependence of the power spectrum. The three-component seismograms from a given station are rotated azimuthally and then by inclination, using, for example the transformation described by Plešinger *et al.* (1986). The power spectrum for a specific direction can then be calculated from the rotated seismogram for that direction.

In a polar plot where the azimuth gives the angle and the radius is proportional to the frequency, the gray shades give the power spectral amplitude (fig. 6). Here it is possible to observe the polarization at several frequencies at the same time. Figure 6 shows the polarization in the horizontal plane for the first seven harmonics at all four Lascar stations. It is apparent that the polarization at a given station is different for each line.

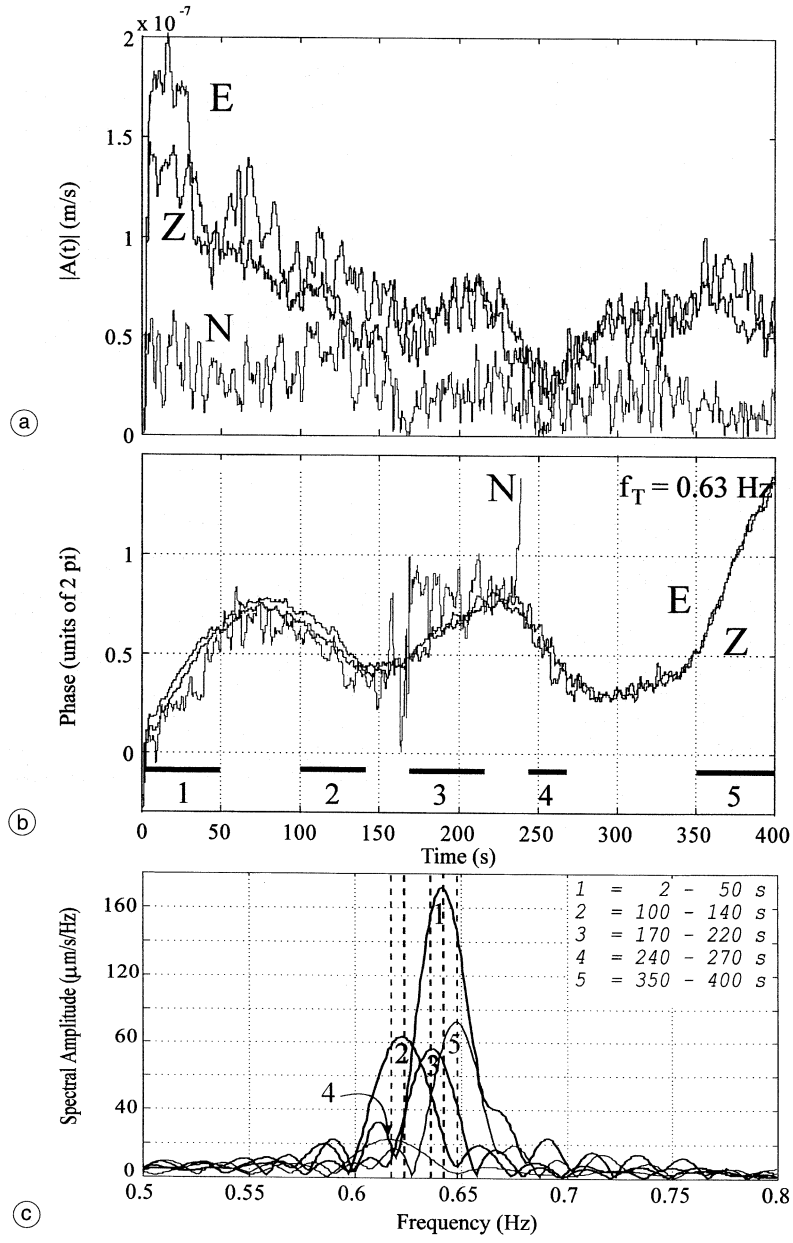

Fig. 7a-c. Hilbert transform of the fundamental (BP filter 0.5-0.9 Hz) at station LA2 for the 400 s interval beginning at 02:35:20 on 18 April 1994. a) Instantaneous amplitude. b) Reduced Instantaneous Phase (RIP), test frequency f_T = 0.63 Hz. c) Determination of the exact frequency of the fundamental for 5 intervals using the amplitude spectrum. The spectra were calculated from data series which were extended with zeros to 50 000 points. The frequency step for the spectra is then df = 0.001 Hz. The vertical dotted lines indicate the frequencies for the chosen intervals calculated using the Hilbert transform.

3.3. *The Hilbert-transform*

The Hilbert-transform of a real function of time, $x(t)$, is

$$y(t) = \mathcal{H}(x(t)) = \frac{1}{\pi} P \int_{-\infty}^{\infty} \frac{x(\xi)}{\xi - t} d\xi \qquad (3.1)$$

where ξ is an integration variable for the time and P is the principal value of the integral (Buttkus, 1991). The analytic function is then defined as

$$z(t) = A(t)e^{i\Theta(t)} = x(t) - iy(t) = x(t) - i\mathcal{H}(x(t)), \qquad (3.2)$$

where $|A(t)|$ is called the instantaneous amplitude and $\Theta(t)$ is the instantaneous phase. Dziewonski and Hales (1972), for example, used this function to determine the group and phase velocities of surface waves. The time derivative of the instantaneous phase is the instantaneous angular frequency:

$$\omega(t) = 2\pi f(t) = \frac{d\Theta(t)}{dt}. \qquad (3.3)$$

The Hilbert transform of a simple sine function, $x(t) = \sin(2\pi f_T t)$, is $y(t) = \cos(2\pi f_T t)$. Its instantaneous phase is then a linear function of time with the slope $2\pi f_T$. For a narrowband signal we can use this fact to observe and measure even the smallest changes in frequency. If, for example, $s(t)$ is a recorded, narrowband signal with an amplitude, $A_1(t)$, and frequency, $f_1(t)$, which both vary with time, we can write

$$s(t) = A_1(t) \sin(2\pi f_1(t)t). \qquad (3.4)$$

If the changes of $f_1(t)$ are small, we can observe them by plotting the reduced instantaneous phase (RIP), $\Theta(t) - 2\pi f_T t$, as a function of time. When $f_1(t) = f_T$, the slope, m, of this curve will be zero. For intervals with constant slope, $f_1(t)$ is constant, and

$$f_1(t) = f_T + m/(2\pi) \qquad (3.5)$$

while changes in $f_1(t)$ are reflected by changes in the slope.

For an interval 400 s long, the instantaneous amplitude of the fundamental, $A_1(t)$, and the RIP at station LA2 are plotted in fig. 7a,b. The instantaneous amplitudes for the Z and E components are similar, while that of the N component is much smaller for the entire interval. Aside from small variations, the RIP are the same for Z and E. During the first 150 s the RIP of the N component also follows the other two. It varies more, however because the signal-to-noise ratio is much lower than for Z and E. This leads, for example at $t = 170$ s, to jumps of 2π. After 250 s such jumps cause the RIP for the N component to wander out of the plot.

For a quantitative analysis of the RIP of the Z and E components we can divide the curve in fig. 7b into five segments with relatively constant slopes ($2 < t < 50$ s, $100 < t < 140$ s, $170 < t < 220$ s, $240 < t < 270$ s and $350 < t < 400$ s). Between these regions, the slope changes. Using eq. (3.5) we can calculate the difference between the actual frequency and the test frequency f_T. Table III compares the RIP results with frequencies determined from a high resolution calculation of the amplitude spectra of the chosen intervals (fig. 7c).

Aside from noise problems, the application of this method to the seismograms of the other

Table III. Frequency variation of harmonic tremor.

Interval	Δf (Hz)	$f_1(t)$ (Hz)	f_s (Hz)
2-50 s	0.0117 + 0.0001	0.642	0.641
100-140 s	– 0.0074 + 0.0005	0.623	0.622
170-220 s	0.0065 + 0.0004	0.636	0.636
240-270 s	– 0.0131 + 0.0023	0.617	0.617
350-400 s	0.0180 + 0.0007	0.648	0.648

stations yields similar results: the polarizations and amplitudes during each of the marked intervals change, yet the frequency of the fundamental remains constant and has exactly the same value at all stations. Similar analysis of the overtones demonstrates that, within the limits of the precision, the overtone frequencies are integer multiples of the fundamental.

4. Discussion

The power spectra of the harmonic tremor at the four Lascar stations have peaks at the same frequencies, which can be given by the relationship $f_n = nf_1$ (fig. 2a,b). Since the paths from the source to the stations as well as the stations' underground are different, the oscillations must be produced at or near the physical source and cannot be explained by path or site effects. Thus the frequency of the harmonic tremor is a characteristic of the source. Further investigation of the frequency of the fundamental and the overtones using the methods developed here gives greater detail.

A comparison of the width of the spectral peaks in the power spectra with the observations of frequency variation made using the Hilbert transform demonstrates that for harmonic tremor, the peak widths are determined by variations of the frequency as a function of time rather than by the «quality» of the resonator (fig. 7a-c). Also, to the precision of measurement (about 0.01 Hz), the frequencies of the overtones, even up to the order n = 20, are exactly integer harmonics of the fundamental. For a physical resonator, as opposed to a theoretical one, this is highly unusual.

When harmonic overtones are present, as at Lascar, it is often assumed that they are generated by higher order resonances of some linear resonant body, such as a flute or organ pipe (Schlindwein *et al.*, 1995) or conceivably a rectangular crack of appropriate dimensions (Chouet, 1996). The wavelengths associated with the overtone resonances are, however, shorter than that of the fundamental. For a realistic physical resonator such as a volcanic flue, the characteristic length sampled by the overtones would be different from the fundamental, particularly for large n. Thus, the frequencies of the overtones would not follow the formula $f_n = nf_1$ as can be observed here. In addition, physical resonators rarely produce more than four or five harmonics. The overtones present in the harmonic tremor records can be explained as a resonance at a single, varying frequency whose amplitude exceeds the range for which the assumptions of linear acoustics are valid (*i.e.* $v_{max} > 0.1$ c). In the rock such large amplitudes would result in small fractures rather than harmonic tremor, implying that the tremor source must be in the volcanic fluids and gases.

The frequency of the harmonic tremor at Lascar varies both on large (fig. 3) and small (fig. 7b) scales. It is possible that such variations are caused by rapid changes in the speed of sound along the path, by the Doppler effect due to motion of the source toward or away from the station, or by changes in the frequency radiated by the source. The first two causes are unlikely, since the source-station directions are very different for the four Lascar stations. Changes in the speed of sound or the Doppler effect should affect waves traveling in different directions differently. The rapid and reversible frequency changes (fig. 7a-c) are also another indication that the source cannot be the resonance of a body such as a crack or organ-pipe-like flue.

There are a number of physical models compatible with the know conditions in volcanoes which produce very large, nonlinear amplitudes. Thermoacoustic oscillators produce extremely high levels of sound in simple heat exchangers (Atchley *et al.*, 1990). A nearly continuous sequence of shock waves due to a constriction in a conduit of flowing liquids could also generate harmonic tremor (Faber, 1995). Small changes in the frequency would indicate slight changes in the flow conditions. Leighton (1994) demonstrates that under certain circumstances the oscillation of bubbles can produce signals with overtones similar to those of harmonic tremor. Other non-linear fluid flow conditions may also generate harmonic ground motion (Julian, 1994).

In earthquake seismology, the type of a wave (P, S_V, S_H, ...) can be determined from its polarization at a single station if the location of the

source is known. Conversely, given the type of wave, we can determine the direction to the source. With four three-component stations, polarization analysis should therefore provide some insight into the wave type and the source. For the harmonic tremor recorded at Lascar, neither short-term (fig. 4a-c) nor long-term (figs. 5 and 6) polarization patterns at the four stations can be reconciled with a single source radiating a single type of wave. In addition, the polarization is different for each harmonic. While the complexity of the polarization may be generated at the sources, it can also be explained by any or all of three simple models models for the medium:

– the polarization of the wavefield is the result of scattering along the paths between the source and the receivers, with different frequencies affected differently (Ingard, 1988);

– the waves are a superposition of narrowband *P* and *S* waves continuously being generated at the source; or

– the polarization at each station is a result of reflections at the surface (Nuttli, 1961; Nuttli and Whitmore, 1961).

Without further measurements, the effects of these processes on the wavefield cannot be distinguished from each other or from any source effect. In any case, unlike the analysis of first arrivals in earthquake seismology, the polarization of the harmonic tremor cannot be used as an indication of the direction to the tremor source.

On the other hand, the polarization remains relatively constant for long intervals, as demonstrated in figs. 5 and 6. If the polarization of the recorded waves is influenced by any or all of the effects described above, this implies that the path between the source and the receivers does not change or changes only very little during the analysis interval. Thus, the tremor source does not change its position during this time.

5. Conclusions

These observations of harmonic tremor at Lascar underscore the importance of high-resolution, three-component recordings from more than one station for volcano-seismological measurements. In contrast to single-component networks, these three-component observations demonstrate that the amplitudes at the measuring site are probably most affected by path, while the frequency and signal phase of narrowband signals retain information about the source.

There is a clear, close relationship between the frequencies of the fundamental and the overtones in that the peaks in the power spectra are extremely sharp and the «nuances» of frequency change follow each other so precisely. This indicates that the overtones are produced not as higher resonances of some resonant body resembling a flute or organ pipe. Rather that the source must be some resonance at a single, varying frequency whose amplitude exceeds the range for which the assumptions of linear acoustics are valid (*i.e.* $v_{max} > 0.1$ c). The source of this oscillation must lie within the magma, magma/gas or gas parts of the volcano, since such large amplitudes in the rock would result in small fractures rather than harmonic tremor. Possible physical models for a source satisfying these observations are the thermoacoustic oscillator (Atchley *et al.*, 1990), shock waves (Faber, 1995), bubble oscillation (Leighton, 1994), or fluid flow effects (Julian, 1994).

Acknowledgements

PISCO'94 was part of the Sonderforschungsbereich 276, «*Deformationprozesse in den Anden*». The SFB is sponsored by the Deutsche Forschungsgemeinschaft and located at the Freie Universität Berlin (Sprecherhochschule), in cooperation with the Technische Universität Berlin, the GeoForschungsZentrum Potsdam and the Universität Potsdam. I particularly thank Günter Asch, who supplied me with the data, and Alex Rudloff and Frank Gräber, without whose efforts this data set would not exist. Suggestions from Rolf Schick, Dieter Seidl and Horst Rademacher went a long way towards improving the manuscript. I would also like to thank Gilberto Saccorotti for his comments and suggestions.

REFERENCES

ANDRES, R.J. and A.D. KASGNOC (1998): A time-averaged inventory of subaerial volcanic sulfur emissions, *J. Geophys. Res.*, **103**, 25251-25261.

ASCH, G., G. BOCK, F. GRÄBER, C. HABERLAND, M. HELLWEG, R. KIND, A. RUDLOFF and K. WYLLAGALLA (1995): Passive Seismologie im Rahmen von PISCO'94, in *Sonderforschungsbereich 267 Deformationsprozesse in den Anden, Berichtband für die Jahre 1993-1995,* Berlin, 619-677.

ASCH, G., K. WYLEGALLA, M. HELLWEG, D. SEIDL and H. RADEMACHER (1996): Observations of rapid-fire event tremor at Lascar volcano, Chile, *Ann. Geofis.,* **39** (2), 273-282.

ATCHLEY, A.A., H.E. BASS and T.J. HOFLER (1990): Development of nonlinear waves in a thermoacoustic prime mover, in *Proceedings of the 12th ISNA «Frontiers of Nonlinear Acoustics»*, edited by M.F. HAMILTON and D.T. BLACKSTOCK (Elsevier Science Publishers Ltd., London), 603-608.

BENOIT, J.P. and S.R. MCNUTT (1997): New constraints on source processes of volcanic tremor at Arenal volcano, Costa Rica, using broadband seismic data, *Geophys. Res. Let.*, **24**, 449-452.

BUTTKUS, B. (1991): *Spektralanalyse und Filtertheorie* (Springer Verlag, Berlin), pp. 650.

CHOUET, B. (1996): New methods and future trends in seismological volcano monitoring, in *Monitoring and Mitigation of Volcano Hazards*, edited by R. SCARPA and R. TILLING (Springer-Verlag, Heidelberg), 23-97.

DZIEWONSKI, A.M. and A.L. HALES (1972): Numerical analysis of dispersed seismic waves, in *Methods in Computational Physics*, edited by B. BOLT (Academic Press, New York), 39-85.

FABER, T.E. (1995): *Fluid Dynamics for Physicists* (Cambridge University Press, Cambridge), pp. 440.

GARDEWEG, M. and E. MEDINA (1994): La erupcion subpliniana del 19-20 de Abril de 1993 del volcan Lascar, N. de Chile, in *Actas del 7. Congreso Geologico Chileno 1994*, vol. 1, 299-304.

GIL-CRUZ, F. (1997): Observations of two special kinds of tremor at Galeras volcano, Colombia (1989-1991), *Ann. Geofis.*, **42** (3), 437-449 (this volume).

HELLWEG, M., D. SEIDL, S.B. KIRBANI and W. BRÜSTLE (1994): Team investigates activity at Mt. Semeru, Java, volcano. *Eos, Trans. Am. Geophys. Un.*, **75**, 313-317.

INGARD, K.U. (1988): *Fundamentals of Waves and Oscillations* (Cambridge University Press, Cambridge), pp. 595.

JULIAN, B.R. (1994): Volcanic tremor: nonlinear excitation by fluid flow, *J. Geophys. Res.*, **99**, 11859-11877.

LEES, J.J., J. JOHNSON, E. GORDEEV, K. BATEREAU and A. OZEROV (1997): Volcanic explosions at Karymsky: a broadband experiment around the Cone, *Eos, Trans. Am. Geophys. Un.*, **78** (46), Fall Meeting Suppl., F430.

LEIGHTON, T.G. (1994): *The Acoustic Bubble* (Academic Press, London), pp. 614.

MATSUMURA, S. (1981): Three-dimensional expression of seismic particle motions by the trajectory ellipsoid and its application to the seismic data observed in the Kanto district, Japan, *J. Phys. Earth*, **29**, 221-239.

MCNUTT, S.R. (1996): Seismic monitoring and eruption forecasting of volcanoes: a review of the state-of-the-art and case histories, in *Monitoring and Mitigation of Volcano Hazards*, edited by R. SCARPA and R. TILLING (Springer-Verlag, Heidelberg), 99-146.

NUTTLI, O. (1961): The effect of the Earth's surface on the *S* wave particle motion, *Bull. Seismol. Soc. Am.*, **51**, 237-246.

NUTTLI, O. and J.D. WHITMORE (1961): An observational determination of the variation of the angle of incidence of *P* waves with epicentral distance, *Bull. Seismol. Soc. Am.*, **51**, 269-276.

PLEŠINGER, A., M. HELLWEG and D. SEIDL (1986): Interactive high-resolution polarization analysis of broadband seismograms, *J. Geophysics*, **59**, 129-139.

SCHLINDWEIN, V., J. WASSERMANN and F. SCHERBAUM (1995): Spectral analysis of harmonic tremor signals at Mt. Semeru volcano, Indonesia, *Geophys. Res. Lett.*, **22**, 1685-1688.

SEIDL, D. and M. HELLWEG (1991): Volcanic tremor recordings: polarization analysis, in *Volcanic Tremor and Magma Flow*, edited by R. SCHICK and R. MUGIONO (Kernforschungsanlage Jülich, Germany), 31-46.